

The ABL due to a Mountain Pass and Coriolis Effect

B. Grisogono¹, L. Enger² and D. Belušić¹

¹Dept. of Geophysics, Fac. of Sci. & Math., Horvatovac bb, Univ. of Zagreb, 10⁴ Zagreb, Croatia.

²Dept. of Earth Sci., Villav. 16, Univ. of Uppsala, S-75646 Uppsala, Sweden.

Email: bgrisog@gfz.hr

Abstract: Idealized airflow over a mountain with a pass is studied using a numerical mesoscale model with a trustful higher-order turbulence parameterization scheme. A uniformly stratified inflow of 8 m/s over mountain, 100km x 20km x 1km, yields Froude number 0.6, while Rossby number along the flow ranges from 7.6 to infinity. A pass drops the mountain top to ~ 400m locally increasing Froude number and modifying the overall wave breaking and the ABL. In the presence of the Earth rotation, $f \neq 0$, which already breaks the lee-side flow symmetry, the pass induces additional variations in the ABL extending far from the mountain. Both, the rotation and the pass, alter the low-level jet structure and the specific humidity field. This mesoscale process may stretch to synoptic scale within a reasonable time, say 15-25h, only when the rotation is included. Otherwise, a somewhat similar process with $f=0$ might take unreasonably long time.

Key words: Wave-breaking, Coriolis, Low-level jet, Turbulence, Mountain waves, Numerical model.

1. INTRODUCTION

We have entered exploring Coriolis effects in the mesoscale, $f \neq 0$, in nonlinear regime only during the last decade (Ólafsson and Bougeault 1997, Enger and Grisogono 1998, Hunt et al. 2001). While the linear theory tells the f -effect is moderately important for mesoscale mountain waves, somewhat enhancing the dispersion and modulating the amplitudes, nonlinear orographic flows exhibit richer flow regimes with $f \neq 0$ (Grisogono and Enger 2004, Hunt et al. 2004). Namely, adding a linear component to a nonlinear system yields a nonlinear response. Thus, linear theory cannot explain the effect of $f \neq 0$ in the presence of significant orographic wave breaking. The latter implicitly means the terrain length perpendicular to the flow, over which the wave breaking occurs, is comparable to Rossby radius.

This study continues on Gaberšek and Durran (2004), addressing idealized gap flows with $f=0$, and on Grisogono and Enger (2004, henceforth GE04) tackling atmospheric boundary layer (ABL) variations due to wave breaking and $f \neq 0$. Here the only change from GE04 is cutting a mountain pass.

2. MODEL AND ITS SETUP

The model used is a version of the MIUU mesoscale numerical model of Enger (1990). It has been reported in a few dozens of scientific papers (e.g. Abiodun and Enger 2002). It employs a faithful scheme for turbulence parameterization (Andrén 1990), and a decent numerical advection scheme of a third order, $O[(\Delta t)^3, (\Delta x)^3]$, see Enger and Grisogono (1998). It is a 3D, time dependent, nonlinear model.

The setup and initialization is the same as in GE04 and is shortly repeated now. The domain is covered by 121x101x36 grid points in (x,y,z) with $\Delta x=2.5\text{km}$, $\Delta y=5\text{km}$ and variable $4\text{m} \leq \Delta z \leq 500\text{m}$; time step $\Delta t=20\text{s}$. The model top is at 15km where a sponge layer occupies the uppermost 5km. Also, the lateral boundary conditions minimize reflections, and no-slip lower boundary condition is used. Temperature at the surface varies only with surface height, not in time, $T(z=0)=280\text{K}$. The constant meteorological input is $(U,V)=(8,0)\text{ms}^{-1}$ with constant buoyancy frequency so that for the mountain top of 1km Froude number is 0.6; Rossby number is ∞ or 7.6. Terrain is an elongated Gaussian mountain 20km wide and 100km long; when the pass is present, it goes to the minimum height of 400m and its characteristic width is 20km. The decrease of already low specific humidity with height assures the latter may be treated as a passive tracer thus aiding the mapping of the ABL. With some imagination, the terrain with the pass can be an idealization

of the mountain of Velebit if north and south are replaced. The roughness length is everywhere 0.1m.

3. RESULTS AND DISCUSSION

Four runs are presented in four figures. Each figure depicts same fields from the four runs: the upper panels show $f=0$ (a,b), the lower panels show $f=10^{-4}\text{s}^{-1}$ (c,d); left panels have no mountain pass, right panels have the pass. The left panels relate to GE04. Figure 1 displays the horizontal wind 95m above the ground level (AGL) after 20h; U is colored, V is in back curves, 1ms^{-1} increments (positive solid, negative dashed, 0 suppressed), the terrain is in white curves (0.1, 0.5 and 1km). Relative strengthening of the northern low-level jet (LLJ) with $f>0$ is obvious; this is relatively enhanced when the pass exists, Fig.1d.

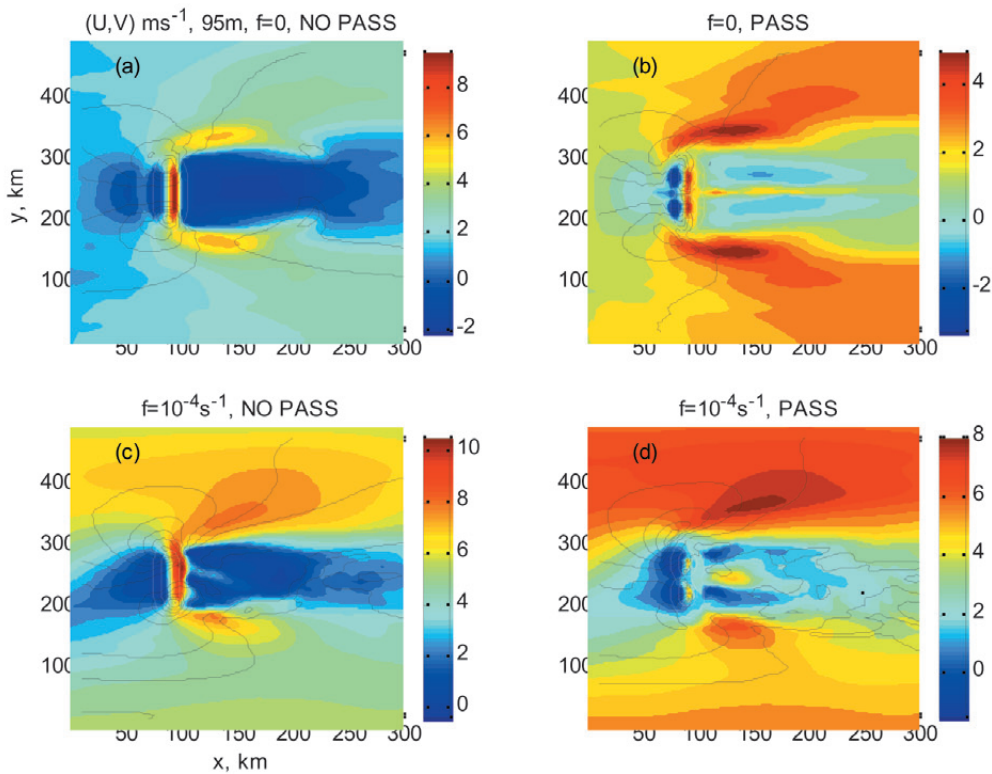


Figure 1. The U (colored) and V-component (black) in the ABL after 20h. The terrain is white. With $f \neq 0$ the ABL is horizontally asymmetric and inhomogeneous; the northern LLJ intensifies.

Both the partial upstream blocking and even more the lee side wind field are affected by $f \neq 0$ and the pass. The lee effect stretches out over the synoptic scale as flow meandering (Hunt et al. 2001). A sign of intensive wave breaking aloft is seen as shooting flow in the lee, $90\text{km} < x < 100\text{km}$ Fig. 1a,b,c; Fig. 1d shows instead a LLJ behind the pass. The wave breaking is non-locally related to the strong lee-side divergence and vorticity additionally coupled via $f \neq 0$ (GE04); this is a negative nonlinear feedback.

The specific humidity, almost a passive tracer here, and turbulent kinetic energy (TKE), colors and curves respectively, are shown in Fig. 2. These fields map the ABL. The lower southern ABL is more humid than its northern counterpart; this reverses in the upper ABL (not shown) as in GE04. This is a consequence of the wind field, and the LLJ in particular, interacting also with the TKE. For our $U>0$, $f>0$ there is more shear driven turbulence around the stronger, northern LLJ, Figs. 1c,d, 2,c,d. Temporal variability in the lee of the mountain is displayed in Fig. 3 showing the TKE and wind direction, colors and curves respectively. The chosen point is at the line of mountain symmetry, $y=250\text{km}$. The model spin-up takes the first few hours. Lee side eddies promote the time variations shown, especially in Fig. 3a,c while in Fig. 3b,d it is the

LLJ due to the pass dictating the TKE evolution.

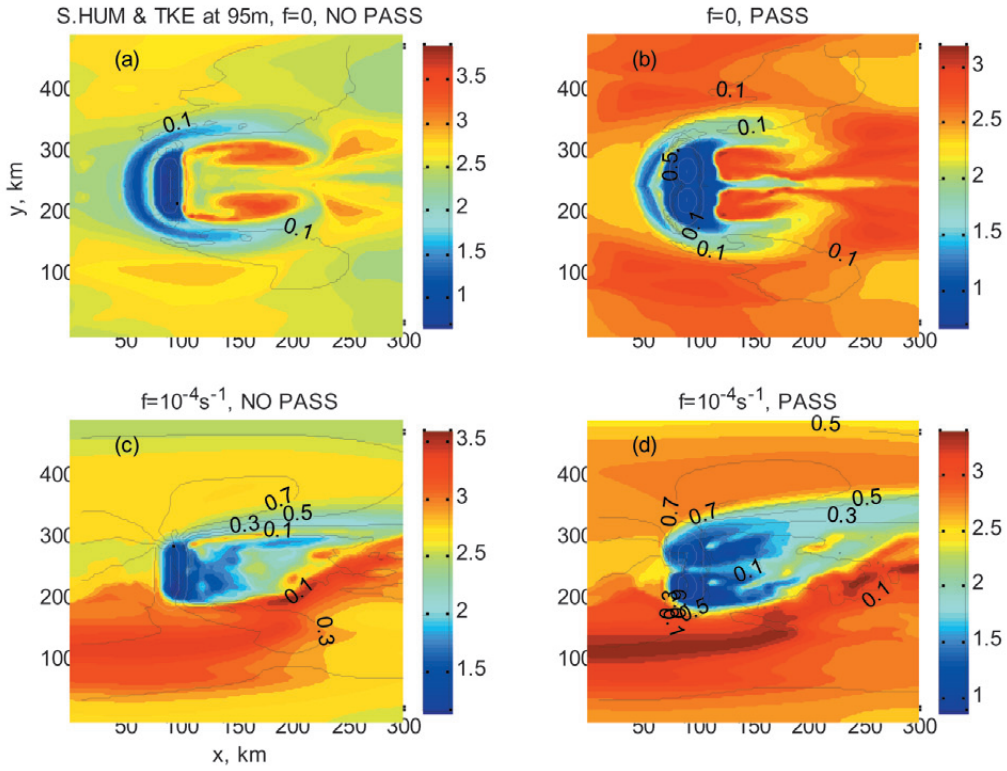


Figure 2. Same as Fig.1 but for the specific humidity, g kg^{-1} , and TKE, m^2s^{-2} , colors and curves respectively. The ABL in c) and d) extend further in the lee than in a) and b).

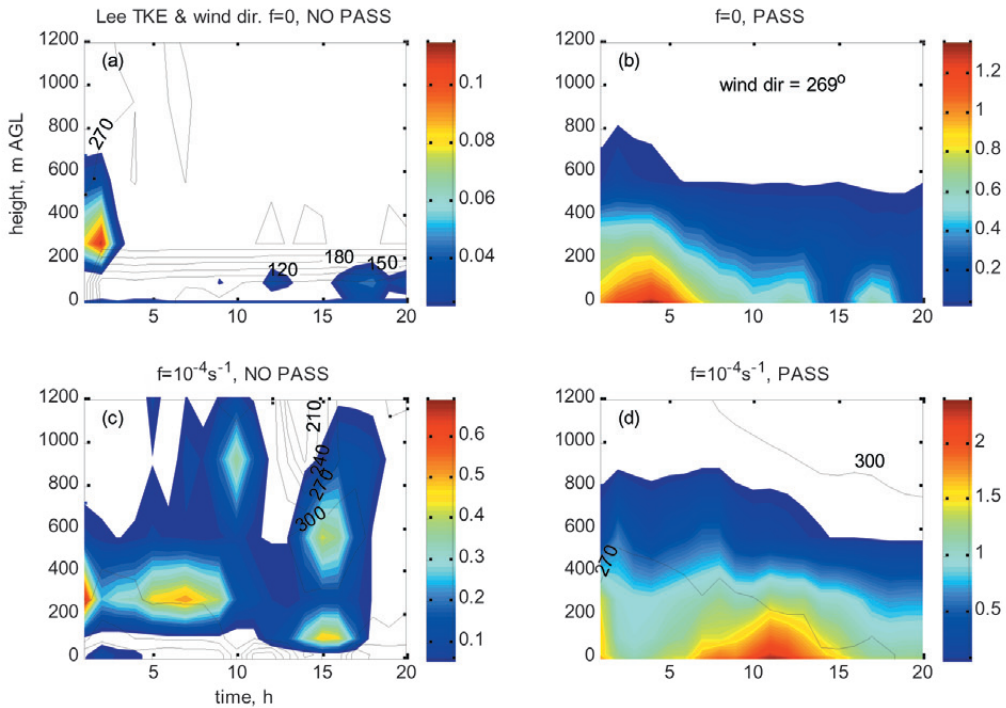


Figure 3. TKE(t,z), m^2s^{-2} , and wind direction, deg, at $(x,y)=(107.5,250)\text{km}$ and 75m above 0 height; the panels correspond to those in Fig.1. Wind direction shown in 30deg increments.

4. CONCLUSIONS

Idealized nonlinear numerical simulations using MIUU mesoscale model are shown for an idealized mountain with and without a pass. The structure of the lower ABL is addressed in four simulations. The rotation, $f \neq 0$, couples i) local but intensive mesoscale wave-breaking induced divergence and vorticity with ii) synoptic scale vorticity and divergence as a nonlinear negative feedback process. This yields the lee side flow meandering and unsteadiness. Hence, $f \neq 0$, and then the pass as well, has a larger influence on the mesoscale dynamics than linear theory and ordinary scale analysis suggest. All this relates to Froude number less than one and Rossby number larger than one.

The lee-side ABL becomes horizontally inhomogeneous and anisotropic over many distances much greater than the mountain size. This may have significant consequences on the low level cloud formation and air chemistry. Finally, if the input $U > 0$ is reversed to $U < 0$, the presence of $f > 0$ is a secondary explanation of why the bura (bora) wind over Velebit mountain, Croatia, is generally stronger at its southern flank, e.g. around Maslenica.

REFERENCES

- Andrén, A., 1990: Evaluation of a turbulence closure scheme suitable for air-pollution applications. *J. Appl. Meteor.* **29**, 224-239.
- Enger, L., 1990: Simulation of dispersion in moderately complex terrain -Part A. The fluid dynamics model. *Atmos. Environ.* **24A**, 2431-2446.
- Enger, L. and B. Grisogono, 1998: The response of bora-type flow to sea surface temperature. *Quart. J. Roy. Meteorol. Soc.* **124**, 1227-1244.
- Gaberšek, S. and D.R. Durran, 2004: Gap flows through idealized topography. Part I: forcing by large-scale winds in the nonrotating limit. *J. Atmos. Sci.* **61**, 2846-2862.
- Grisogono, B. and L. Enger, 2004: Boundary-layer variations due to orographic wave-breaking in the presence of rotation. *Quart. J. Roy. Meteorol. Soc.*, **130**, 2991-3014. (abbrev. GE04)
- Hunt, J.C.R., H. Ólafsson and P. Bougeault, 2001: Coriolis effects on orographic and mesoscale flows. *Quart. J. Roy. Meteorol. Soc.* **127**, 601-633.
- Hunt, J.C.R., A. Orr, J.W. Rottmann and R. Capon, 2004: Coriolis effects in mesoscale flows with sharp changes in surface conditions. *Quart. J. Roy. Meteorol. Soc.* **130**, 2703-2731.
- Ólafsson, H. and P. Bougeault, 1997: The effect of rotation and surface friction on orographic drag. *J. Atmos. Sci.* **54**, 193-210.